ELSEVIER

Journal of Physics and Chemistry of Solids 63 (2002) 197–202

JOURNAL OF PHYSICS AND CHEMISTRY OF SOLIDS

www.elsevier.com/locate/jpcs

Temperature dependence of impurity quenched luminescence in Tm^{3+}:$LiLuF_4$

F. Cornacchia[a], L. Palatella[a], A. Toncelli[a], M. Tonelli[a,*], A. Baraldi[b], R. Capelletti[b], E. Cavalli[c], K. Shimamura[d], T. Fukuda[d]

[a]*INFM-Dipartimento di Fisica dell'Università di Pisa, Via Buonarroti, 2, 56127 Pisa, Italy*
[b]*INFM-Dipartimento di Fisica dell'Università di Parma, Parco Area delle Scienze 7/A, 43100 Parma, Italy*
[c]*Dipartimento di Chimica Generale ed Inorganica, Chimica Analitica, Chimica Fisica, dell'Università di Parma, Parco Area delle Scienze 17/A, 43100 Parma, Italy*
[d]*Institute for Materials Research, Tohoku University, Sendai 980-8577, Japan*

Received 14 December 2000; accepted 10 April 2001

Abstract

The study of the optical properties of a $LiLuF_4$ crystal doped with Tm^{3+} yielded the discovery of a strong temperature dependence of the Tm–Tm diffusion coefficient. Spectroscopic characteristics have been investigated as a function of the sample temperature, with particular regard to the luminescence decay following pulsed excitation. An appreciable excitation of the lifetime of the $^3F_4$ manifold is observed over the temperature range 8.9–298 K. The Judd–Ofelt calculations point out a radiative lifetime considerably longer than the experimental one. These facts suggest a theoretical interpretation based on the presence of impurities that quench the manifold and on a temperature-dependent energy migration between Tm^{3+} ions. A one-parameter best fit of the experimental measurements strongly confirms this hypothesis. Weak OH^- ion concentration is detected by means of IR and UV spectra, thus supporting the theoretical interpretation.

Keywords: A. Optical materials; D. Luminescence; D. Optical properties

1. Introduction

The aim of this work is to investigate the optical properties of a Tm^{3+}:$LiLuF_4$ crystal with particular insight in the $^3F_4 \rightarrow {}^3F_4$ migration process.

The interest in Tm^{3+} ions is based on the possibility of obtaining laser action in the visible and infrared wavelength regions, in particular in the 1.8 μm region in the case of single-doped crystals and in the 2 μm region in the case of crystals co-doped with Ho^{3+}. The laser action has been obtained in a wide variety of host crystals pumped with flash lamps, ion lasers or diode lasers and with operating temperatures extending from 77 K to room temperature both in pulsed and cw regime [1]. In order to study the feasibility of such devices, it is necessary to measure the optical characteristics of the sample: in particular the absorption and fluorescence spectra. Other important parameters to evaluate the possibility of obtaining laser action are the lifetime of the upper laser level and the emission cross-section of the laser transition ($^3F_4 \rightarrow {}^3H_6$ in the case of 1.8 μm lasers with Tm^{3+} ions).

The phenomenon of the lifetime temperature dependence is generally related to phonon relaxation [2], but, if this is the case, the behavior of the lifetime is characterized by a rather weak and smooth variation as a function of temperature [3]. Moreover, the $^3F_4$ lifetime at room temperature is typically a few milliseconds in oxide crystals and about 10 ms in fluorides [4]. On the contrary, in the sample under investigation, an abrupt decrease of the $^3F_4$ lifetime (about 70% between 8.9 and 50 K) and a room temperature lifetime ≈ 2 ms have been observed. This behavior is very similar to that of, for example, $Eu(PO_3)_3$ with Cr impurities [5] and of Tb:$Y_3Al_5O_{12}$ with Si and Ca impurities [6]. This work extends the theoretical interpretation given in Ref. [5] to the case of Tm-doped fluoride crystals and envisages the impurities as responsible for the lifetime shortening.

* Corresponding author. Tel.: +39-050-844336; fax: +39-050-844333.
E-mail address: tonelli@df.unipi.it (M. Tonelli).

0022-3697/01/$ - see front matter
PII: S0022-3697(01)00129-9

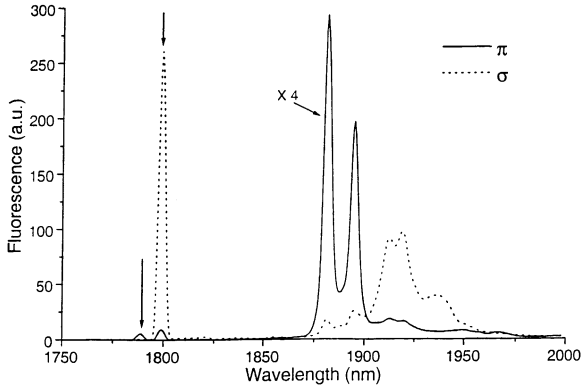

Fig. 1. 10 K polarized fluorescence spectra of $^3F_4$ manifold; $\lambda_{exc} = 791.9$ nm.

The main result is that the Tm–Tm energy migration can undergo an abrupt change at a particular temperature depending on the host crystal features. So, the knowledge of this phenomenon can be important in the development of laser crystals based on Tm–Tm energy migration such as Tm–Ho lasers.

2. Experimental details

The $LiLuF_4$ crystal is an isomorph to the well known $LiYF_4$ (YLF), and, therefore, belongs to the tetragonal system with C_{4h}^6-$I4_1$ symmetry. The lattice parameters are $a = b = 0.5167$ nm and $c = 1.0375$ nm. Rare earths substitute for Lu^{3+} ions in sites with S_4 symmetry [7].

The sample under investigation has been grown by the Czochralski method at the Institute for Materials Research of Tohoku University, Sendai (Japan). The nominal Tm^{3+} concentration is 10 wt%, corresponding to 1.4×10^{21} ions cm^{-3}. The sample used is a parallelepiped of $5.5 \times 6.0 \times 2.2$ mm^3 with polished surfaces.

Absorption measurements between 185 and 2000 nm were performed at room temperature by means of a CARY 500 spectrophotometer with a resolution as good as 0.1 nm up to 830 nm and 0.4 nm further on. Absorption measurements in the range 4000–500 cm^{-1} (2.5–20 μm) were performed at 9 K by means of a Bomem DA8 FTIR spectrophotometer, with a resolution as good as 0.02 cm^{-1}. The sample was assembled in a closed-cycle CTI cryo-cooler.

Room temperature fluorescence spectra were measured by exciting the sample with a cw tunable Ti:Al_2O_3 laser. The power incident on the sample could be varied between 20 and 85 mW. The pump wavelength was tuned to a maximum in the absorption of the $^3H_6 \rightarrow {}^3H_4$ Tm^{3+} transition. The signal from the sample was focused on the input slit of a 25 cm monochromator with spectral resolution of 3 nm. The radiation was detected by a cooled InSb detector. The signal from the detector was processed by a lock-in amplifier, and stored on a PC. The optical response of the system was normalized for the two polarizations in the range of interest.

For the fluorescence decay curves, the sample was mounted on the cold finger of a closed-cycle cryo-cooler and the temperature could be varied from 8.9 to 298 K. The pump beam was mechanically chopped and the power incident on the crystal was only 7 mW, in order to eliminate any non-linear effect. Moreover, the crystal was pumped near an edge and the fluorescence was collected from a thin section (≈ 1 mm) of the sample. The signal from the InSb detector was processed by a digital oscilloscope. The system response time was 0.17 ms, fast enough to measure the 10-ms order of magnitude of the lifetime of the $^3F_4$ manifold.

3. Fluorescence measurements and impurity investigation

We measured the polarized absorption spectra in the region 400–2000 nm at 300 K. The spectra are typical of Tm-doped crystals and do not show any unusual feature; the most interesting band is at 800 nm, because it lies in the emission region of powerful commercial diode lasers. The sample was pumped by the Ti:Al_2O_3 at 792 nm with $E \| c$ polarization. The absorption coefficient at this wavelength is $\alpha = 9$ cm^{-1}. The $^3F_4$ manifold is then populated by means of a cross-relaxation process.

Fig. 1 displays the π and σ polarized 10 K fluorescence spectra of the $^3F_4 \rightarrow {}^3H_6$ transition. The aim of this measurement is to study the splitting of the ground manifold $^3H_6$ into its Stark sublevels, because, at 10 K only the lowest sublevel of the $^3F_4$ manifold is populated. The analysis of the spectra leads to the determination of the energy position of the sublevels: 0, 31, 273, 313, 360, 379, 381, 427, (503) cm^{-1} (the last value is uncertain), in agreement with the values of Tm^{3+}:YLF reported in the literature [8].

A theoretical model to evaluate the transition probabilities between rare earth manifolds is that developed by Judd

Table 1
Lifetime vs temperature. The lifetime experimental error is 0.17 ms

Temperature (K)	Lifetime (ms)
8.9	7.05
10.1	6.45
12.1	5.53
15	4.61
20.1	3.63
25	3.06
30	2.74
40	2.25
50	1.97
76.9	1.70
139.7	1.87
199.9	1.82
298	1.65

and Ofelt [9] which allows the intensity parameters Ω_λ ($\lambda = 2, 4, 6$) to be obtained from the room temperature absorption spectra.

These calculations were performed taking into account the magnetic dipole correction for the $^3H_6 \rightarrow {}^3H_5$ transition and using the reduced matrix elements taken from Ref. [1]. The intensity parameters obtained are:

$$\Omega_2 = 2.12 \times 10^{-20}\ \mathrm{cm}^2, \qquad \Omega_4 = 1.17 \times 10^{-20}\ \mathrm{cm}^2, \qquad \Omega_6 = 1.11 \times 10^{-20}\ \mathrm{cm}^2, \tag{1}$$

and the relative RMS is $0.16 \times 10^{-20}\ \mathrm{cm}^2$. Following the method of Refs. [1,9] it is possible to evaluate the theoretical radiative lifetime of the various multiplets. For $^3F_4$, the lifetime is $\tau_R = 9.4 \pm 2.3$ ms.

This theoretical result is similar to the corresponding values theoretically and experimentally obtained for other fluoride crystals, for example YLF, doped with Tm^{3+} [1,4].

Using the experimental apparatus described in Section 2, the $^3F_4$ manifold lifetime was measured; the results are shown in Table 1. All the observed decay curves were single exponential within experimental accuracy, which implies the absence of non-linear phenomena. Nevertheless, the most significant feature of the measurements is the strong temperature dependence of the $^3F_4$ level lifetime. In fact, not only is the lifetime shorter than the theoretical one, but it abruptly decreases as the temperature changes from 8.9 to 50 K, and does not change significantly from 50 K up to room temperature. A 3 K change in the crystal temperature causes a 20% variation of the lifetime: this behavior cannot be explained by phonon relaxation because the energy of this transition ($\approx 5000\ \mathrm{cm}^{-1}$) is much higher than the typical phonon energy of fluoride crystals ($\hbar\omega \approx 400$–$500\ \mathrm{cm}^{-1}$) [10].

This fact suggests the presence of impurities with energy levels approximately resonant with the Tm transitions, which should quench in a non-radiative way the $^3F_4$ level.

Possible candidates are OH^- ions. In fact, it is widely known that one of the most difficult problems when growing fluoride crystals is to avoid the presence of OH^- ions in the melt because they can cause luminescence quenching [11–13]. OH^- ions usually substitute for F^- ions in fluoride crystals [14] and give rise to electronic absorption in UV [15] and vibrational ones in IR. Therefore, the absorption spectra in the range 186–225 nm (see Fig. 2) and in the range 3000–4000 cm^{-1} (see Fig. 3) were measured at 300 and 9 K, respectively. Fig. 2 displays a main peak at 212 nm with a FWHM of 5.2 nm and a weaker one at $\approx$ 192 nm, while Fig. 3 shows a narrow line at 3621.3 cm^{-1} with a FWHM of 1.7 cm^{-1}. The absorption at 212 nm (≈ 5.85 eV) falls in the electronic absorption range for OH^- in alkali halides (from 9 eV in LiF to 5.2 eV in KCl). For such simple systems, the peak shifts towards lower energies as the lattice constant increases and the ionic character decreases [15]. In the case of fluorides, the OH^- electronic absorption falls at high energy (8–9 eV) for the simplest ones, such as LiF and NaF, but occurs at lower energies for the more complex ones, such as $KMgF_3$ (6.62 eV) [16]. Therefore, the attribution of the 212 nm peak displayed in Fig. 2 to OH^- ions seems reasonable, considering that $LiLuF_4$ is a rather complex fluoride and the lattice constant is appreciably larger at least in one direction than that of LiF and NaF (0.4–0.5 nm).

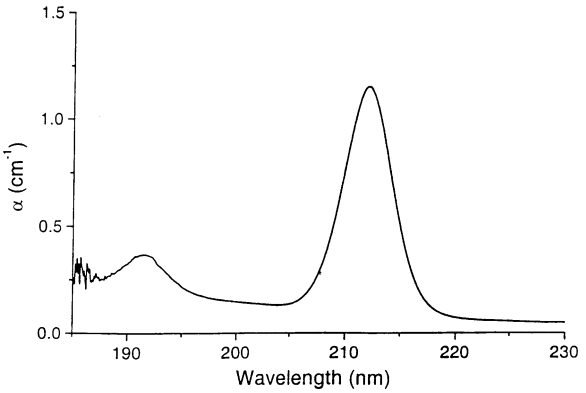

Fig. 2. Room temperature UV-absorption spectrum.

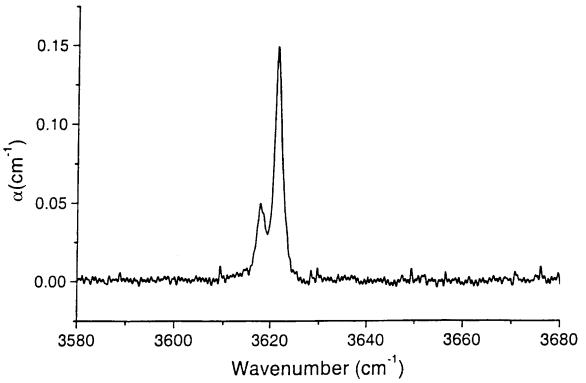

Fig. 3. IR absorption spectrum measured at 9 K.

The weak peak detected in IR at 3621.3 cm^{-1}, i.e. in the region of the fundamental OH^- stretching modes [16,17], provides a further support to the above attribution in agreement with Ref. [18]. Assuming for the OH^- stretching mode transition in $LiLuF_4$ the same oscillator strength as determined experimentally by Guckelsberger [19] for OH^- in LiF, a rough evaluation of the OH^- concentration in $LiLuF_4$ can be easily obtained from the absorption coefficient at the peak ($\alpha = 0.15\ cm^{-1}$) and from the FWHM ($1.7\ cm^{-1}$) at 9 K. The value so estimated is $\approx 6 \times 10^{16}$ ions cm^{-3}, corresponding to ≈ 40 ppm with respect to Tm concentration.

4. Theoretical interpretation

In this section, a theoretical explanation is provided for the peculiar behavior of the lifetime versus crystal temperature.

As a first step, the energy of the $^3F_4$ Tm level is assumed to migrate from ion to ion until it arrives in the neighborhood of an impurity (e.g. OH^-) that absorbs it and then decays in a non-radiative way. Such a process has already been studied and shown to occur in the general case of crystals containing both energy acceptor and donor dopants [5], but has never been applied to fluorides. In general, the donor excitation density ϕ obeys the equation:

$$\frac{\partial}{\partial t}\phi(\vec{r},t) = D\nabla^2\phi(\vec{r},t) - \sum_a \nu(\vec{r}-\vec{r}_a)\phi(\vec{r},t) - \frac{1}{\tau_R}\phi(\vec{r},t), \tag{2}$$

where D is the diffusion coefficient, τ_R is the radiative lifetime and $\nu(\vec{r}-\vec{r}_a)$ is the probability per unit of time that the energy is transferred from a donor (Tm^{3+}) to an acceptor (impurity).

The acceptor concentration is very low, as estimated in the previous section, consequently, the donor–donor transfer probability is much higher than the donor–acceptor one. Moreover, if the acceptor lifetime is very short compared with the donor one the time evolution of ϕ undergoes an exponential decay with an effective lifetime τ:

$$\frac{1}{\tau} = \frac{1}{\tau_R} + \frac{1}{\tau_D}, \tag{3}$$

where $1/\tau_D$ is the decay rate due to the Tm–Tm migration and subsequent quenching. It should be remarked that a lifetime as short as 7 ns (i.e. much shorter than the Tm^{3+} lifetime) has been reported for the OH^- vibrational decay in KBr [20]. In the hypothesis that the donor–acceptor coupling is of the form $C|\vec{r}-\vec{r}_a|^{-6}$, i.e. a dipole–dipole interaction, that is the most probable between the two species, the diffusive lifetime can be written as:

$$\frac{1}{\tau_D} = 8.5 N_a C^{1/4} D(T)^{3/4}, \tag{4}$$

where N_a is the acceptor concentration and T the crystal temperature.

The experimental data of $^3F_4$ decay time can be explained by Eqs. (3) and (4). The temperature dependence of the donor–acceptor coupling C is expected to be very small, so, in order to explain the peculiar behavior of the $^3F_4$ lifetime, attention is focused on the temperature dependence of the diffusion coefficient D. As shown in the scheme in Fig. 4, when the temperature increases, the available resonant transfer transition is not only the $(2 \rightarrow 0, 0 \rightarrow 2)$ (thin arrows in the scheme), but also the $(2 \rightarrow 1, 1 \rightarrow 2)$ (thick arrows in the scheme). Fig. 4 also shows the donor–acceptor energy transfer process, due to the dipole–dipole coupling C between the $^3F_4$ manifold and a completely non-radiative quenching impurity level (dashed arrow in the figure).

In this condition, the diffusion coefficient can be expressed in the following form:

$$D \propto \frac{\frac{g_0^2}{g_2}\frac{f_{02}^2}{\nu_{02}^2\Delta\nu_{02}} + \frac{g_1^2}{g_2}\frac{f_{12}^2}{\nu_{12}^2\Delta\nu_{12}} e^{-E_1/k_B t}}{g_0 + g_1 e^{-E_1/k_B t}} = \frac{D_{02} + D_{12} e^{-E_1/k_B t}}{g_0 + g_1 e^{-E_1/k_B t}}, \tag{5}$$

where g_i are the Tm^{3+} Stark sublevel degeneration (in this

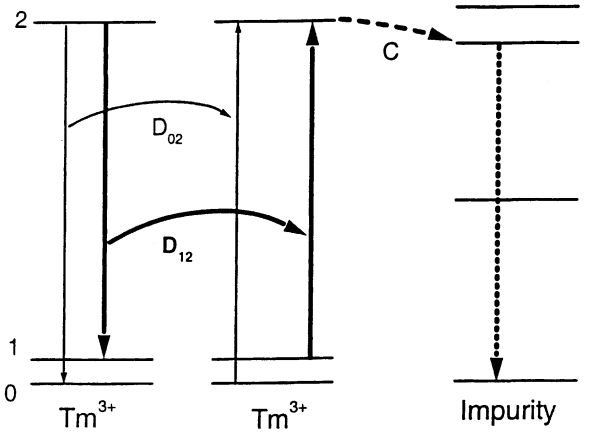

Fig. 4. Energy transfer diagram. The '0' indicates the lowest Stark sublevel of ground state $^3H_6$ and '1' the sublevel found at 31 cm^{-1}, while '2' is the lowest sublevel of $^3F_4$ (not to scale).

case $g_0 = 1$ $g_1 = 2$ $g_2 = 1$) like in YLF [1], $\Delta\nu_{ij}$ are the bandwidths, f_{ij} the related oscillator strengths and E_1 is the energy of the second sublevel of the ground manifold. If the frequencies, the bandwidths, the oscillator strengths and the degeneracies of the two transitions were all equal, D should be temperature independent. In the present case, the ratio between the oscillator strengths of the transitions $2 \rightarrow 0$ at 1789 nm and $2 \rightarrow 1$ at 1799 nm (indicated with arrows in Fig. 1), properly weighted with degeneracies is 1/88, as obtained from the peak ratio of the fluorescence measurements.

Since the bandwidths and the frequencies are approximately the same for the two available transitions, it is possible to write:

$$D \propto \frac{1 + B\mathrm{e}^{-E_1/k_\mathrm{B}t}}{1 + 2\mathrm{e}^{-E_1/k_\mathrm{B}t}}, \tag{6}$$

where B, the ratio between the two different diffusion coefficients, is assumed to be the square of the ratio of the two oscillator strengths and degeneracies (7744). It may be worth noting that the diffusion coefficient is affected by a strong variation when $k_\mathrm{B}T$ reaches the values corresponding to E_1 due to the fact that $f_{12} > f_{02}$ in our crystal.

Considering Eqs. (3), (4), and (6), the decay time τ becomes:

$$\tau = \left[\left(A \frac{1 + B\mathrm{e}^{-E_1/k_\mathrm{B}t}}{1 + 2\mathrm{e}^{-E_1/k_\mathrm{B}t}} \right)^{3/4} + \frac{1}{\tau_R} \right]^{-1}, \tag{7}$$

where A is a suitable dimensional constant taking into account the unknown value of C and of the diffusion coefficient. A one-parameter (A) best fit of the lifetime experimental data was performed using $B = 7744$, $E_1 = 31$ cm^{-1}, and $\tau_R = 9.4$ ms. The values of the first two parameters are obtained experimentally, while the radiative lifetime value is derived from the Judd–Ofelt calculation.

Fig. 5 shows the experimental lifetime results and the one-parameter best fit. The agreement between theoretical

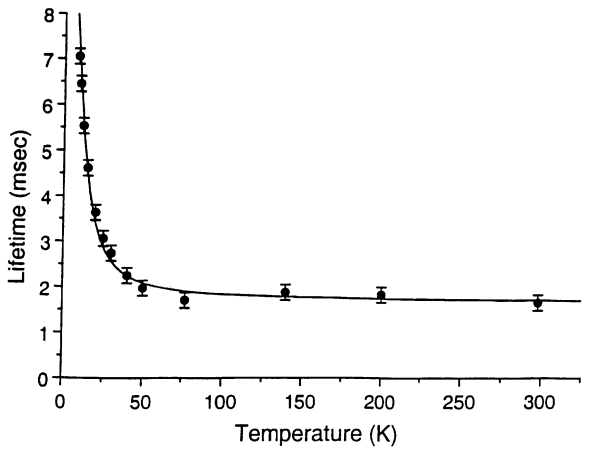

Fig. 5. $^3F_4$ lifetime versus temperature and the best fit curve of Eq. (7).

prediction (Eq. (7)) and experimental data is very good. In fact, at 10 K Tm–Tm diffusion is very small and the probability of energy transfer to a quenching impurity is rather small, while at about 50 K (corresponding to $k_BT \approx 31\ cm^{-1}$) a new and much more efficient channel for diffusion is turned on. From this temperature up to room temperature, the excitation travels through the crystal and, hence, the probability of quenching by an impurity increases and the $^3F_4$ lifetime is shortened.

5. Conclusions

We have shown the absorption spectra in the UV and IR wavelength regions and the static and dynamic fluorescence of $^3F_4 \rightarrow {}^3H_6$ transition in the 1.8 μm region. By means of Judd–Ofelt calculations, we obtained the line strengths and the Ω_λ parameters for Tm^{3+} in $LiLuF_4$ and the theoretical radiative lifetime of the $^3F_4 \rightarrow {}^3H_6$ transition. All these results are in agreement with those of Tm^{3+}:YLF crystals, except for the $^3F_4$ lifetime that has been shown to be strongly temperature dependent.

This behavior was investigated and theoretically explained by means of a model based on a temperature-dependent Tm–Tm energy migration and on the presence of impurities. Therefore, the presence of OH^- impurities led us to discover the main result of this work: in $LiLuF_4$ the Tm–Tm energy migration is strongly temperature dependent (D undergoes a 3-order-of-magnitude change when T varies from 10 to 300 K). This feature is very important because the Tm–Tm energy migration is fundamental in various solid state lasers such as the Tm–Ho laser. Moreover, the abrupt change in the diffusion coefficient happens at ≈ 20 K in our case, but it could take place at a different temperature depending on the host crystal and, in particular, on the energy of the second Stark sublevel of ground manifold.

References

[1] A.A. Kaminskii, Crystalline Lasers: Physical Processes and Operating Schemes, CRC Press, Boca Raton, FL, 1996.
[2] M.J. Weber, Phys. Rev. B 8 (1973) 54.
[3] E. Cavalli, C. Meschini, A. Toncelli, M. Tonelli, M. Bettinelli, J. Phys. Chem. Solids 58 (1997) 587.
[4] S.A. Payne, L.L. Chase, L.K. Smith, W.L. Kway, W.F. Krupke, IEEE J. Quantum Electron. 28 (1992) 2619.
[5] M.J. Weber, Phys. Rev. B 4 (1972) 2932 and references therein.
[6] J.P. van der Ziel, L. Kopf, L.G. van Uitert, Phys. Rev. B 6 (1972) 615.
[7] A.A. Kaminskii, K. Ueda, N. Uehara, Jpn. J. Appl. Phys. 32 (1993) L586.
[8] H.P. Jenssen, A. Linz, R.P. Leavitt, C.A. Morrison, D.E. Wortman, Phys. Rev. B 11 (1975) 92.
[9] B.R. Judd, Phys. Rev. 127 (1962) 750 and also G.S. Ofelt, J. Chem. Phys. 37 (1962) 511.
[10] L.A. Riseberg, H.W. Weber, Relaxation phenomena in rare earth luminescence, in: E. Wolf (Ed.), Progress in Optics XIV, North Holland, Amsterdam-Oxford, 1976.
[11] T.C. Stobe, J. Phys. Chem. Solids 28 (1967) 1375.
[12] G. Blasse, Intern. Rev. Chem. 11 (1992) 71.
[13] L. Gomes, F. Luty, Phys. Rev. B 30 (1984) 7194.
[14] B. Fritz, F. Luty, J. Anger, Z. Phys. 174 (1963) 240.
[15] A. Scacco, C. Marasca, U.M. Grassano, R. Capelletti, S. Prato, N. Zema, J. Physics: Condensed Matter 6 (1994) 7813.
[16] R. Capelletti, A. Baraldi, P. Bertoli, M. Cornelli, U.M. Grassano, A. Ruffini, A. Scacco, in: G. Borstel, A. Krumins, D. Millers (Eds.), Defects and Surface-Induced Effects in Advanced Perovskites, Kluwer Academic, The Netherlands, 2000, pp. 293–304.
[17] R. Capelletti, P. Beneventi, A. Ruffini, Ber. Bunsenges Phys. Chem. 101 (1997) 1265.
[18] I.M. Ranieri, K. Shimamura, K. Nakano, T. Fujita, Z. Liu, N. Sarakura, T. Fukuda, J. Crystal Growth 217 (2000) 151.
[19] K. Guckelsberger, J. Phys. Chem. Sol. 41 (1980) 1209.
[20] E. Gustin, M. Leblans, A. Bouwen, D. Schoemaker, F. Luty, Phys. Rev. B 54 (1996) 6963.